On Self-Approaching and Increasing-Chord Drawings of 3-Connected Planar Graphs

Martin Nöllenburg, Roman Prutkin, and Ignaz Rutter

Institute of Theoretical Informatics, Karlsruhe Institute of Technology, Germany

Abstract. An st-path in a drawing of a graph is self-approaching if during a traversal of the corresponding curve from s to any point t' on the curve the distance to t' is non-increasing. A path has increasing chords if it is self-approaching in both directions. A drawing is self-approaching (increasing-chord) if any pair of vertices is connected by a self-approaching (increasing-chord) path.

We study self-approaching and increasing-chord drawings of triangulations and 3-connected planar graphs. We show that in the Euclidean plane, triangulations admit increasing-chord drawings, and for planar 3-trees we can ensure planarity. Moreover, we give a binary cactus that does not admit a self-approaching drawing. Finally, we show that 3-connected planar graphs admit increasing-chord drawings in the hyperbolic plane and characterize the trees that admit such drawings.

1 Introduction

Finding a path between two vertices is one of the most fundamental tasks users want to solve when considering graph drawings. Empirical studies have shown that users perform better in path-finding tasks if the drawings exhibit a strong geodesic-path tendency [10,17]. Not surprisingly, graph drawings in which a path with certain properties exists between every pair of vertices have become a popular research topic. Over the last years a number of different drawing conventions implementing the notion of strong geodesic-path tendency have been suggested, namely *greedy drawings* [18], *(strongly) monotone drawings* [2], and *self-approaching* and *increasing-chord drawings* [1]. Note that throughout this paper, all drawings are straight-line and vertices are mapped to distinct points.

The notion of greedy drawings came first and was introduced by Rao et al. [18]. Motivated by greedy routing schemes, e.g., for sensor networks, one seeks a drawing, where for every pair of vertices s and t there exists an st-path, along which the distances to t decrease in every vertex. This ensures that greedily sending a message to a vertex that is closer to the destination guarantees delivery. Papadimitriou and Ratajczak conjectured that every 3-connected planar graph admits a greedy embedding into the Euclidean plane [16]. This conjecture has been proved independently by Leighton and Moitra [13] and Angelini et al. [5]. Kleinberg [12] showed that every connected graph has a greedy drawing in the hyperbolic plane. Eppstein and Goodrich [7] showed how to construct such an embedding, in which the coordinates of each vertex are represented using only $O(\log n)$ bits, and Goodrich and Strash [9] provided a corresponding *succinct* representation for greedy embeddings of 3-connected planar graphs in $\mathbb{R}^2$. Angelini et al. [3] showed that some graphs require exponential area for a greedy drawing in $\mathbb{R}^2$. Wang and He [21] used a custom distance metric to construct planar, convex and succinct greedy embeddings of 3-connected planar graphs using Schnyder realizers [20]. Nöllenburg and Prutkin [14] characterized trees admitting a Euclidean greedy embedding. However, a number of interesting questions remain open, e.g., whether every 3-connected planar graph admits a planar and convex Euclidean greedy embedding (strong Papadimitriou-Ratajczak conjecture [16]). Regarding planar greedy drawings of triangulations, the only known result is an existential proof by Dhandapani [6].

While getting closer to the destination, a greedy path can make numerous turns and may even look like a spiral, which hardly matches the intuitive notion of geodesic-path tendency. To overcome this, Angelini et al. [2] introduced monotone drawings, where one requires that for every pair of vertices s and t there exists a *monotone path*, i.e., a path that is monotone with respect to some direction. Ideally, the monotonicity direction should be $\overrightarrow{st}$. This property is called *strong monotonicity*. Angelini et al. showed that biconnected planar graphs admit monotone drawings [2] and that plane graphs admit monotone drawings with few bends [4]. The existence of strongly monotone planar drawings remains open, even for triangulations.

Both greedy and monotone paths may have arbitrarily large *detour*, i.e., the ratio of the path length and the distance of the endpoints can, in general, not be bounded by a constant. Motivated by this fact, Alamdari et al. [1] recently initiated the study of *self-approaching* graph drawings. Self-approaching curves, introduced by Icking [11], are curves where for any point t' on the curve, the distance to t' decreases continuously while traversing the curve from the start to t'. Equivalently, a curve is self-approaching if, for any three points a, b, c in this order along the curve, it is $\text{dist}(a, c) \geq \text{dist}(b, c)$, where dist denotes the Euclidean distance. An even stricter requirement are so-called *increasing-chord* curves, which are curves that are self-approaching in both directions. The name is motivated by the characterization of such curves, which states that a curve has increasing chords if and only if for any four distinct points a, b, c, d in that order, it is $\text{dist}(b, c) \leq \text{dist}(a, d)$. Self-approaching curves have detour at most 5.333 [11] and increasing-chord curves have detour at most 2.094 [19]. Alamdari et al. [1] studied the problem of recognizing whether a given graph drawing is self-approaching as well as connecting given points to a self-approaching drawing. They also gave a complete characterization of trees admitting self-approaching drawings.

We note that every increasing chord drawing is self-approaching and strongly monotone [1]. The converse is not true. A self-approaching drawing is greedy, but not necesserily monotone, and a greedy drawing is generally neither self-approaching nor monotone. For trees, the notions of self-approaching and increasing-chord drawing coincide.

Contribution. We obtain the following results on constructing self-approaching or increasing-chord drawings.

1. We show that every triangulation has an increasing-chord drawing (answering an open question of Alamdari et al. [1]) and construct a *binary cactus* that does not admit a self-approaching drawing (Sect. 3). The latter is a notable difference to greedy drawings since both constructions of greedy drawings for 3-connected planar graphs [5, 13] essentially show that every binary cactus has a greedy drawing.

2. We show how to construct plane increasing-chord drawings for *planar 3-trees* (a special class of triangulations) using Schnyder realizers (Sect. 4). To the best of our knowledge, this is the first construction for this graph class, even for greedy and strongly monotone plane drawings, which addresses an open question of Angelini et al. [2].
3. We show that, similarly to the greedy case, the hyperbolic plane $\mathbb{H}^2$ allows representing a broader class of graphs than $\mathbb{R}^2$ (Sect. 5). We prove that a tree has a self-approaching or increasing-chord drawing in $\mathbb{H}^2$ if and only if it either has maximum degree 3 or is a subdivision of $K_{1,4}$ (this is not the case in $\mathbb{R}^2$; see the characterization by Alamdari et al. [1]), implying every 3-connected planar graph has an increasing-chord drawing. We also show how to construct planar increasing-chord drawings of binary cactuses in $\mathbb{H}^2$.

2 Preliminaries

For points $a, b, c, d \in \mathbb{R}^2$, let ray$(a, b)$ denote the ray with origin a and direction $\overrightarrow{ab}$ and ray$(a, \overrightarrow{bc})$ the ray with origin a and direction $\overrightarrow{bc}$. Let dir(ab) be the vector $\overrightarrow{ab}$ normalized to unit length. Let $\angle(\overrightarrow{ab}, \overrightarrow{cd})$ denote the smaller angle formed by the two vectors $\overrightarrow{ab}$ and $\overrightarrow{cd}$. For an angle $\alpha \in [0, 2\pi]$, let R_α denote the rotation matrix $\left(\begin{smallmatrix}\cos\alpha & -\sin\alpha \\ \sin\alpha & \cos\alpha\end{smallmatrix}\right)$.

For vectors $\overrightarrow{v_1}, \overrightarrow{v_2}$ with dir$(\overrightarrow{v_2}) = R_\alpha \cdot$ dir$(\overrightarrow{v_1})$, $\alpha \in [0, 2\pi)$, we write $\angle_{\text{ccw}}(\overrightarrow{v_1}, \overrightarrow{v_2}) := \alpha$. Further, let $[\overrightarrow{v_1}, \overrightarrow{v_2}]$ denote the *cone of directions* $\{\overrightarrow{v} \mid \text{dir}(\overrightarrow{v}) = R_\beta \cdot \text{dir}(\overrightarrow{v_1}), \beta \in [0, \alpha]\}$. Let $|[\overrightarrow{v_1}, \overrightarrow{v_2}]| := \alpha$ be its *size*. For a set of directions D, let $\overline{D}$ denote a minimum cone of directions containing D, and let $|D| = |\overline{D}|$. Note that if $|D| < 180°$, $\overline{D}$ is unique.

We reuse some notation from the work of Alamdari et al. [1]. For points $p, q \in \mathbb{R}^2, p \neq q$, let l^+_{pq} denote the halfplane not containing p bounded by the line through q orthogonal to the segment pq. A piecewise-smooth curve is self-approaching if and only if for each point a on the curve, the line perpendicular to the curve at a does not intersect the curve at a later point [11]. This leads to the following characterization of self-approaching paths.

Fact 1 (Corollary 2 in [1]). *Let $\rho = (v_1, v_2, \ldots, v_k)$ be a directed path embedded in $\mathbb{R}^2$ with straight-line segments. Then, ρ is self-approaching if and only if for all $1 \leq i < j \leq k$, the point v_j lies in $l^+_{v_i v_{i+1}}$.*

We shall denote the reverse of a path ρ by ρ^{-1}. Let $\rho = (v_1, v_2, \ldots, v_k)$ be a self-approaching path. Define $\text{front}(\rho) = \bigcap_{i=1}^{k-1} l^+_{v_i v_{i+1}}$, see also Fig. 1. Using Fact 1, we can decide whether a concatenation of two paths is self-approaching.

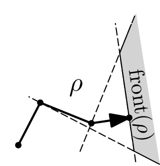

Fig. 1: self-approaching path ρ and front(ρ).

Fact 2. *Let $\rho_1 = (v_1, \ldots, v_k)$ and $\rho_2 = (v_k, v_{k+1}, \ldots, v_m)$ be self-approaching paths. The path $\rho_1.\rho_2 := (v_1, \ldots, v_k, v_{k+1}, \ldots, v_m)$ is self-approaching if and only if $\rho_2 \subseteq \text{front}(\rho_1)$.*

A path ρ has *increasing chords* if for any points a, b, c, d in this order along ρ, it is dist$(b, c) \leq$ dist(a, d). A path has increasing chords if and only if it is self-approaching in both directions. The following result is easy to see.

Lemma 1. *Let $\rho = (v_1, \ldots, v_k)$ be a path such that for any $i < j$, $i, j \in \{1, \ldots, k-1\}$, it is $\angle(\overrightarrow{v_i v_{i+1}}, \overrightarrow{v_j v_{j+1}}) \leq 90°$. Then, ρ has increasing chords.*

Let $G = (V, E)$ be a connected graph. A *separating k-set* is a set of k vertices whose removal disconnects the graph. A vertex forming a separating 1-set is called *cutvertex*. A graph is *c-connected* if it does not admit a separating k-set with $k \leq c - 1$; 2-connected graphs are also called *biconnected*. A connected graph is biconnected if and only if it does not contain a cutvertex. A *block* is a maximal biconnected subgraph. The *block-cutvertex tree* (or *BC-tree*) T_G of G has a *B-node* for each block of G, a *C-node* for each cutvertex of G and, for each block ν containing a cutvertex v, an edge between the corresponding B- and C-node. We associate B-nodes with their corresponding blocks and C-nodes with their corresponding cutvertices.

The following notation follows the work of Angelini et al. [5]. Let T_G be rooted at some block ν containing a non-cutvertex (such a block ν always exists). For each block $\mu \neq \nu$, let $\pi(\mu)$ denote the *parent block* of μ, i.e., the grandparent of μ in T_G. Let $\pi^2(\mu)$ denote the parent block of $\pi(\mu)$ and, generally, $\pi^{i+1}(\mu)$ the parent block of $\pi^i(\mu)$. Further, we define the *root* $r(\mu)$ of μ as the cutvertex contained in both μ and $\pi(\mu)$. Note that $r(\mu)$ is the parent of μ in T_G. In addition, for the root node ν of T_G, we define $r(\nu)$ to be some non-cutvertex of ν. Let $\text{depth}_B(\mu)$ denote the number of B-nodes on the $\nu\mu$-path in T_G minus 1, and let $\text{depth}_C(r(\mu)) = \text{depth}_B(\mu)$. If μ is a leaf of T_G, we call it a *leaf block*.

If every block of G is outerplanar, G is called a *cactus*. In a *binary* cactus every cutvertex is part of exactly two blocks. For a binary cactus G with a block μ containing a cutvertex v, let G_μ^v denote the maximal connected subgraph containing v but no other vertex of μ. We say that G_μ^v is a *subcactus* of G.

A cactus is *triangulated* if each of its blocks is internally triangulated. A *triangular fan with vertices $V_t = \{v_0, v_1, \ldots, v_k\}$ and root v_0* is a graph on V_t with edges $v_i v_{i+1}$, $i = 1, \ldots, k-1$, as well as $v_0 v_i$, $i = 1, \ldots, k$. Let us consider a special kind of triangulated cactuses, each of whose blocks μ is either an edge or a *triangular fan* with root $r(\mu)$. We call such a cactus *downward-triangulated* and every edge of a block μ incident to $r(\mu)$ a *downward* edge.

For a fixed straight-line drawing of a binary cactus G, we define sets $U(G) = \{\overrightarrow{r(\mu)v} \mid \mu \text{ is a block of } G \text{ containing } v,\ v \neq r(\mu)\}$ and $D(G) = \{\overrightarrow{uv} \mid \overrightarrow{vu} \in U(G)\}$, i.e. the sets of *upward* and *downward* directions of G.

3 Graphs with Self-Approaching Drawings

A natural approach to construct (not necessarily plane) self-approaching drawings is to construct a self-approaching drawing of a spanning subgraph. For instance, to draw a graph G containing a Hamiltonian path H with increasing chords, we simply draw H consecutively on a line. In this section, we consider 3-connected planar graphs and the special case of triangulations, which addresses an open question of Alamdari et al. [1]. These graphs are known to have a spanning binary cactus [5, 13]. Angelini et al. [5] showed that every triangulation has a spanning downward-triangulated binary cactus.

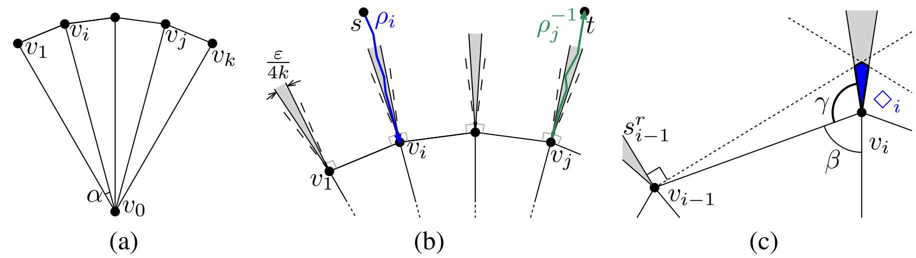

Fig. 2: Drawing a triangulated binary cactus with increasing chords inductively. The drawings $\Gamma_{i,\varepsilon'}$ of the subcactuses, $\varepsilon' = \frac{\varepsilon}{4k}$, are contained inside the gray cones. It is $\beta = 90° - \varepsilon'$, $\gamma = 90° + \varepsilon'/2$.

3.1 Increasing-chord drawings of triangulations

We show that every downward-triangulated binary cactus has an increasing-chord drawing. The construction is similar to the one of the greedy drawings of binary cactuses in the two proofs of the Papadimitriou-Ratajczak conjecture [5, 13]. Our proof is by induction on the height of the BC-tree. We show that G can be drawn such that all downward edges are almost vertical and the remaining edges almost horizontal. For vertices s, t, an st-path with increasing chords goes downwards to some block μ, then sideways to another cutvertex of μ and, finally, upwards to t. Let $\overrightarrow{e_1}, \overrightarrow{e_2}$ be vectors $(1, 0)^\top$, $(0, 1)^\top$.

Theorem 1. *Let $G = (V, E)$ be a downward-triangulated binary cactus. For any $0° < \varepsilon < 90°$, there exists an increasing-chord drawing Γ_ε of G, such that for each vertex v contained in some block μ, $v \neq r(\mu)$, the angle formed by $\overrightarrow{r(\mu)v}$ and $\overrightarrow{e_2}$ is at most $\frac{\varepsilon}{2}$.*

Proof. Let G be rooted at block ν. As our base case, let $\nu = G$ be a triangular fan with vertices $v_0, v_1, \ldots, v_k$ and root $v_0 = r(\nu)$. We draw v_0 at the origin and distribute $v_1, \ldots, v_k$ on the unit circle, such that $\angle(\overrightarrow{e_2}, \overrightarrow{v_0 v_1}) = k\alpha/2$ and $\angle(\overrightarrow{v_0 v_i}, \overrightarrow{v_0 v_{i+1}}) = \alpha$, $\alpha = \varepsilon/k$; see Fig. 2a. By Lemma 1, path $(v_1, \ldots, v_k)$ has increasing chords.

Now let G have multiple blocks. We draw the root block ν, $v_0 = r(\nu)$, as in the previous case, but with $\alpha = \frac{\varepsilon}{2k}$. Then, for each $i = 1, \ldots, k$, we choose $\varepsilon' = \frac{\varepsilon}{4k}$ and draw the subcactus G_i rooted at v_i inductively, such that the corresponding drawing $\Gamma_{i,\varepsilon'}$ is aligned at $\overrightarrow{v_0 v_i}$ instead of $\overrightarrow{e_2}$; see Fig 2b. Note that ε' is the angle of the cones (gray) containing $\Gamma_{i,\varepsilon'}$. Obviously, all downward edges form angles at most $\frac{\varepsilon}{2}$ with $\overrightarrow{e_2}$.

We must be able to reach any t in any G_j from any s in any G_i via an increasing-chord path ρ. To achieve this, we make sure that no normal on a downward edge of G_i crosses the drawing of G_j, $j \neq i$. Let Λ_i be the cone with apex v_i and angle ε' aligned with $\overrightarrow{v_0 v_i}$, $v_0 \notin \Lambda_i$ (gray regions in Fig. 2b). Let s_i^l and s_i^r be the left and right boundary rays of Λ_i with respect to $\overrightarrow{v_0 v_i}$, and h_i^l, h_i^r the halfplanes with boundaries containing v_i and orthogonal to s_i^l and s_i^r respectively, such that $v_0 \in h_i^l \cap h_i^r$. Define $\Diamond_i = \Lambda_i \cap h_{i-1}^r \cap h_{i+1}^l$ (thin blue quadrangle in Fig. 2c), and analogously $\Diamond_j$ for $j \neq i$. It holds $\Diamond_j \subseteq h_i^r \cap h_i^l$ for each $i \neq j$. We now scale each drawing $\Gamma_{i,\varepsilon'}$ such that it is contained in $\Diamond_i$. In particular, for any downward edge uv in $\Gamma_{i,\varepsilon'}$, we have $\Gamma_{j,\varepsilon'} \subseteq \Diamond_j \subseteq l_{uv}^+$ for $j \neq i$. We claim that the resulting drawing of G is an increasing-chord drawing.

Consider vertices s,t of G. If s and t are contained in the same subgraph G_i, an increasing-chord st-path in G_i exists by induction. If s is in G_i and t is v_0, let ρ_i be the sv_i-path in G_i that uses only downward edges. By Lemma 1, path ρ_i is increasing-chord and remains so after adding edge $v_i v_0$.

Finally, assume t is in G_j with $j \neq i$. Let ρ_j be the tv_j-path in G_j that uses only downward edges. Due to the choice of ε', $h_i^r \cap h_i^l \subseteq \mathrm{front}(\rho_i)$ contains $v_1, \ldots, v_k$ in its interior. Consider the path $\rho' = (v_i, v_{i+1}, \ldots, v_j)$. It is self-approaching by Lemma 1; also, $\rho' \subseteq \mathrm{front}(\rho_i)$ and $\rho_j \subseteq \mathrm{front}(\rho')$. It also holds $\rho_j \subseteq \Diamond_j \subseteq \mathrm{front}(\rho_i)$. Fact 2 lets us concatenate ρ_i, ρ' and ρ_j^{-1} to a self-approaching path. By a symmetric argument, it is also self-approaching in the opposite direction and, thus, is increasing-chord. □

Since every triangulation has a spanning downward-triangulated binary cactus [5], this implies that planar triangulations admit increasing-chord drawings.

Corollary 1. *Every planar triangulation admits an increasing-chord drawing.*

3.2 Non-triangulated cactuses

The above construction fails if the blocks are not triangular fans since we now cannot just use downward edges to reach the common ancestor block. Consider the family of rooted binary cactuses $G_n = (V_n, E_n)$ defined as follows. Graph G_0 is a single 4-cycle, where an arbitrary vertex is designated as the root. For $n \geq 1$, consider two disjoint copies of G_{n-1} with roots a_0 and c_0. We create G_n by adding new vertices r_0 and b_0 both adjacent to a_0 and c_0; see Fig. 3a. For the new block ν containing r_0, a_0, b_0, c_0, we set $r(\nu) = r_0$. We select r_0 as the root of G_n and ν as its root block. For a block μ_i with root r_i, let a_i, b_i, c_i be its remaining vertices, such that $b_i r_i \notin E_n$. For a given drawing, due to the symmetry of G_n, we can rename the vertices a_i and c_i such that $\angle_{\text{ccw}}(\overrightarrow{r_i c_i}, \overrightarrow{r_i a_i}) \leq 180°$. We now prove the following negative result.

Theorem 2. *For $n \geq 9$, G_n has no self-approaching drawing.*

The outline of the proof is as follows. We show that every self-approaching drawing Γ of G_9 contains a self-approaching drawing of G_3 with the following properties.
1. If μ_i is contained in the subcactus rooted at c_j, each self-approaching $b_i a_j$-path uses edge $b_i a_i$, and analogously for the symmetric case; see Lemma 5.
2. Each block is drawn significantly smaller than its parent block; see Lemma 6(i).
3. If the descendants of block μ form subcactuses G_k with $k \geq 2$ on both sides, the parent block of μ must be drawn smaller than μ; see Lemma 6(ii).

Obviously, the second and third conditions are contradictory. The following lemmas will be used to show that the drawings of certain blocks must be relatively thin, i.e., their downward edges have similar directions; see the full version for the omitted proofs [15].

Lemma 2. *For cactus $G = (V, E)$ and $s, t \in V$, consider cutvertices $v_1, \ldots, v_k$ lying on any st-path in G in this order. Then, the path $(s, v_1, \ldots, v_k, t)$ is drawn greedily, i.e., each of its subpaths is greedy. In particular,* $\mathrm{ray}(v_1, s)$ *and* $\mathrm{ray}(v_k, t)$ *diverge.*

Obviously, this divergence property also holds for a self-approaching drawing of any cactus. From now on, we consider a fixed self-approaching drawing Γ of G_9. For

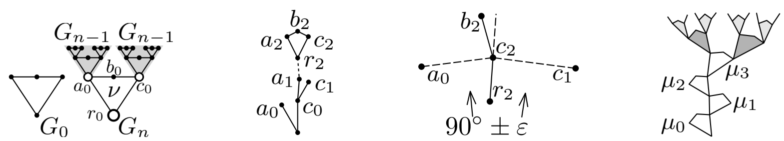

(a) (b) (c) (d)

Fig. 3: (a) cactuses G_n; (b),(c) construction for Lemma 5; (d) subcactus G_5 providing the contradiction in the proof of Theorem 2.

a block μ of G_9 with root $r = r(\mu)$, we write G^r for $(G_9)^r_\mu$, i.e., the binary cactus subgraph of G_9 rooted at r. We write U^r for the set of directions of the upward edges of G^r and define $I^r = \overline{U^r}$. Using Lemma 2, we can show that vectors in $U^{a_i} \cup U^{c_i}$ have the following circular order: first vectors in U^{a_i}, then vectors in U^{c_i}. It follows easily: $\min\{|I^{a_i}|, |I^{c_i}|\} < |I^{r_i}|/2$. Thus, we can provide a bound for the smallest of the cones of a subcactus depending on the depth of its root.

Lemma 3. *Every self-approaching drawing of G_9 contains a cutvertex $\bar{r}$ with* $\mathrm{depth}_C(\bar{r}) = 4$ *and* $|I^{\bar{r}}| < 22.5^\circ$.

Let $\bar{r}$ be a cutvertex from Lemma 3 in the fixed drawing, and let $\varepsilon := |I^{\bar{r}}|$. Then, $G^{\bar{r}}$ is isomorphic to G_6. From now on, we only consider non-leaf blocks μ_i and vertices r_i, a_i, b_i, c_i in $G^{\bar{r}}$. We shall sometimes name the points a instead of a_i etc. for convenience. We assume $\angle(\overrightarrow{e_2}, \overrightarrow{ra}), \angle(\overrightarrow{e_2}, \overrightarrow{rc}) < \varepsilon/2$. The following lemma is proved using basic trigonometric arguments.

Lemma 4. *It holds:* (i) $\angle abc \geq 90^\circ$*;* (ii) $G^a \subseteq l^+_{ba}$, $G^c \subseteq l^+_{bc}$*;* (iii) $\angle bar \leq 90^\circ + \varepsilon$, $\angle bcr \leq 90^\circ + \varepsilon$. (iv) *For vertices u in G^a, v in G^c of degree 4 it is $\angle(\overrightarrow{uv}, \overrightarrow{e_1}) \leq \varepsilon/2$.*

We can now describe block angles at a_i, c_i more precisely and characterize certain self-approaching paths in $G^{\bar{r}}$. We show that a self-approaching path from b_i *downwards and to the left*, i.e., to an ancestor block μ_j of μ_i, such that μ_i is in G^{c_j}, must use a_i. Similarly, a self-approaching path *downwards and to the right* must use c_i. Since for several ancestor blocks of μ_i the roots lie on both of these two kinds of paths, we can bound the area containing them and show that it is relatively small. This implies that the ancestor blocks are small as well, providing a contradiction.

Lemma 5. *Consider non-leaf blocks μ_0, μ_1, μ_2, such that $r(\mu_1) = c_0$ and μ_2 in G^{a_1}; see Fig. 3b.* (i) *It is $\angle r_2a_2b_2, \angle r_2c_2b_2 \in [90^\circ, 90^\circ + \varepsilon]$, b_2 lies to the right of* $\mathrm{ray}(r_2, a_2)$ *and to the left of* $\mathrm{ray}(r_2, c_2)$. (ii) *Each self-approaching b_2a_0-path uses a_2; each self-approaching b_2c_1-path uses c_2.*

Proof. (i) Assume $\angle r_2a_2b_2 < 90^\circ$. Then, all self-approaching b_2a_0 and b_2c_1-paths must use c_2. By Lemma 4(iv), the lines through a_0c_2 and c_2c_1 are "almost horizontal", i.e., $\angle(\overrightarrow{a_0c_2}, \overrightarrow{e_1}), \angle(\overrightarrow{c_2c_1}, \overrightarrow{e_1}) \leq \varepsilon/2$. Since r_2c_2 is "almost vertical", r_2 must lie below these lines and it is $\angle a_0c_2r_2, \angle c_1c_2r_2 \in [90^\circ - \varepsilon, 90^\circ + \varepsilon]$; see Fig. 3c. First, let b_2 lie to the left of $\mathrm{ray}(r_2, c_2)$. Then, b_2 is above a_0c_2, and it is $\angle r_2c_2b_2 = \angle a_0c_2r_2 + \angle a_0c_2b_2 \geq$

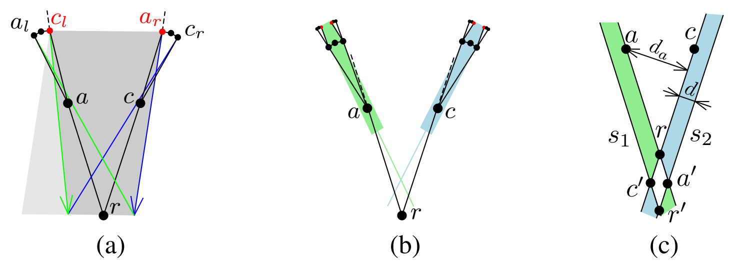

Fig. 4: Showing the contradiction in Theorem 2.

$(90° - \varepsilon) + 90°$. Now let b_2 lie to the right of ray(r_2, c_2). Then, b_2 is above c_2c_1, and it is $\angle r_2c_2b_2 = \angle c_1c_2r_2 + \angle c_1c_2b_2 \geq (90° - \varepsilon) + 90°$. Since $\varepsilon < 22.5°$, this contradicts Lemma 4(iii). Similarly, $\angle r_2c_2b_2 \geq 90°$. Thus, by Lemma 4(iii), $\angle r_2c_2b_2, \angle r_2c_2b_2 \in [90°, 90° + \varepsilon]$. Since $\angle a_2b_2c_2 \geq 90°$, b_2 lies to the right of ray(r_2, a_2) and to the left of ray(r_2, c_2). (If b_2 lies to the left of both rays, it is $\angle a_2b_2c_2 = \angle(\overrightarrow{a_2b_2}, \overrightarrow{c_2b_2}) \leq 2\varepsilon < 90°$.) (ii) Similarly, if a self-approaching b_2a_0-path uses c_2 instead of a_2, it is $\angle r_2c_2b_2 \geq 180° - \varepsilon$. The last part follows analogously. □

From now on, let μ_0 be the root block of $G^{\bar{r}}$ and μ_1, μ_2, μ_3 its descendants such that $r(\mu_1) = c_0$, $r(\mu_2) = a_1$, $r(\mu_3) \in \{a_2, c_2\}$; see Fig. 3d. Light gray blocks are the subject of Lemma 6(i), which shows that several ancestor roots lie inside a cone with a small angle. Dark gray blocks are the subject of Lemma 6(ii), which considers the intersection of the cones corresponding to a pair of sibling blocks and shows that some of their ancestor roots lie inside a narrow strip; see Fig. 4a for a sketch.

Lemma 6. *Let μ be a block in G^{c_2} with vertices a, b, c, $r(\mu)$.* (i) *Let μ have depth 5 in $G^{\bar{r}}$. Then, the cone $l^+_{ba} \cap l^+_{bc}$ contains $r(\mu)$, $r(\pi(\mu))$, $r(\pi^2(\mu))$ and $r(\pi^3(\mu))$.* (ii) *Let μ have depth 4 in $G^{\bar{r}}$. There exist u in G^a and v in G^c of degree 4 and a strip S containing $r(\mu)$, $r(\pi(\mu))$, $r(\pi^2(\mu)) = r(\mu_2)$, such that u and v lie on the different boundaries of S.*

Again, we consider two siblings and the intersection of their corresponding strips, which forms a small diamond containing the root of the ancestor block; see Fig. 4b, 4c.

Lemma 7. *Consider block $\mu = \mu_3$ containing $r = r(\mu), a, b, c$, and let $r_\pi := r(\pi(\mu_3))$. It holds:* (i) $|r_\pi r| \leq \frac{(1+2\tan\varepsilon)(\tan\varepsilon)^2}{\cos\varepsilon}(|ra| + |rc|)$*;* (ii) $|ra|, |rc| \leq |rr_\pi|(\tan\varepsilon)^2$.

For $\varepsilon \leq 22.5°$, the two claims of Lemma 7 contradict each other. This concludes the proof of Theorem 2.

4 Planar Increasing-Chord Drawings of 3-Trees

In this section, we show how to construct planar increasing-chord drawings of 3-trees. We make use of *Schnyder labelings* [20] and drawings of triangulations based on them. For a plane triangulation $G = (V, E)$ with external vertices r, g, b, its Schnyder labeling is an orientation and partition of the interior edges into three trees T_r, T_g, T_b (called *red*, *green* and *blue tree*), such that for each internal vertex v, its incident edges appear in the following clockwise order: exactly one outgoing red, an arbitrary number of incoming blue, exactly one outgoing green, an arbitrary number of incoming red, exactly one outgoing blue, an arbitrary number of incoming green. Each of the three outer vertices r, g, b serves as the root of the tree in the same color and all its incident interior edges are incoming in the respective color. For $v \in V$, let R_v^r (the *red region* of v) denote the region bounded by the vg-path in T_g, the vb-path in T_b and the edge gb. Let $|R_v^r|$ denote the number of the interior faces in R_v^r. The green and blue regions R_v^g, R_v^b are defined analogously. Assigning v the coordinates $(|R_v^r|, |R_v^g|, |R_v^b|) \in \mathbb{R}^3$ results in a plane straight-line drawing of G in the plane $\{x = (x_1, x_2, x_3) \mid x_1 + x_2 + x_3 = f - 1\}$ called *Schnyder drawing*. Here, f denotes the number of faces of G. For a thorough introduction to this topic, see the book of Felsner [8].

For $\alpha, \beta \in [0^\circ, 360^\circ]$, let $[\alpha, \beta]$ denote the corresponding counterclockwise cone of directions. We consider drawings satisfying the following constraints.

Definition 1. *Let $G = (V, E)$ be a plane triangulation graph with a Schnyder labeling. For $0^\circ \leq \alpha \leq 60^\circ$, we call an arbitrary planar straight-line drawing of G α-*Schnyder *if for each internal vertex $v \in V$, its outgoing red edge has direction in $[90^\circ - \frac{\alpha}{2}, 90^\circ + \frac{\alpha}{2}]$, blue in $[210^\circ - \frac{\alpha}{2}, 210^\circ + \frac{\alpha}{2}]$ and green in $[330^\circ - \frac{\alpha}{2}, 330^\circ + \frac{\alpha}{2}]$ (see Fig. 5a).*

According to Def. 1, classical Schnyder drawings are 60°-Schnyder. The next lemma shows an interesting connection between α-Schnyder and increasing-chord drawings.

Lemma 8. *30°-Schnyder drawings are increasing-chord drawings.*

Proof. Let $G = (V, E)$ be a plane triangulation with a given Schnyder labeling and Γ a corresponding 30°-Schnyder drawing. Let r, g, b be the red, green and blue external vertex, respectively, and T_r, T_g, T_b the directed trees of the corresponding color.

Consider vertices $s, t \in V$. First, note that monochromatic directed paths in Γ have increasing chords by Lemma 1. Assume s and t are not connected by such a path. Then, they are both internal and s is contained in one of the regions R_t^r, R_t^g, R_t^b. Without loss of generality, we assume $s \in R_t^r$. The sr-path in T_r crosses the boundary of R_t^r, and we assume without loss of generality that it crosses the blue boundary of R_t^r in $u \neq t$; see Fig. 5b. The other cases are symmetric.

Let ρ_r be the su-path in T_r and ρ_b the tu-path in T_b; see Fig. 5c. On the one hand, the direction of a line orthogonal to a segment of ρ_r is in $[345^\circ, 15^\circ] \cup [165^\circ, 195^\circ]$. On the other hand, ρ_b is contained in a cone $[15^\circ, 45^\circ]$ with apex u. Thus, $\rho_b^{-1} \subseteq \mathrm{front}(\rho_r)$, and $\rho_r.\rho_b^{-1}$ is self-approaching by Fact 2. By a symmetric argument it is also self-approaching in the other direction, and hence has increasing chords. $\square$

Planar 3-trees are the graphs obtained from a triangle by repeatedly choosing a (triangular) face f, inserting a new vertex v into f, and connecting v to each vertex of f.

Lemma 9. *Planar 3-trees have α-Schnyder drawings for any $0^\circ < \alpha \leq 60^\circ$.*

Proof. We describe a recursive construction of an α-Schnyder drawing of a planar 3-tree. We start with an equilateral triangle and put a vertex v in its center. Then, we align

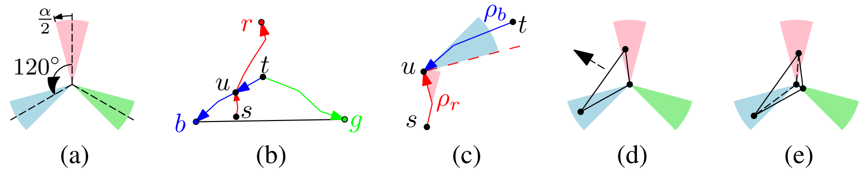

Fig. 5: (a)–(c) 30°-Schnyder drawings are increasing-chord; (d),(e) special case of planar 3-trees.

the pattern from Fig. 5a at v. For the induction step, consider a triangular face xyz and assume that the pattern is centered at one of its vertices, say x, such that the other two vertices are in the interiors of two distinct cones; see Fig. 5d. It is now possible to move the pattern inside the triangle slightly, such that the same holds for all three vertices x, y, z; see Fig. 5e. We insert the new vertex at the center of the pattern and again get the situation as in Fig. 5d. □

Lemmas 8 and 9 provide a constructive proof for the following theorem.

Theorem 3. *Every planar 3-tree has a planar increasing-chord drawing.*

5 Self-Approaching Drawings in the Hyperbolic Plane

Kleinberg [12] showed that any tree can be drawn greedily in the hyperbolic plane $\mathbb{H}^2$. This is not the case in $\mathbb{R}^2$. Thus, $\mathbb{H}^2$ is more powerful than $\mathbb{R}^2$ in this regard. Since self-approaching drawings are closely related to greedy drawings, it is natural to investigate the existence of self-approaching drawings in $\mathbb{H}^2$.

We shall use the *Poincaré disk* model for $\mathbb{H}^2$, in which $\mathbb{H}^2$ is represented by the unit disk $D = \{x \in \mathbb{R}^2 : |x| < 1\}$ and lines are represented by circular arcs orthogonal to the boundary of D. For an introduction to the Poincaré disk model, see e.g. Kleinberg [12] and the references therein.

First, let us consider a tree $T = (V, E)$. A drawing of T in $\mathbb{R}^2$ is self-approaching if and only if no normal on an edge of T in any point crosses another edge [1]. The same condition holds in $\mathbb{H}^2$; see full version for the proof [15]. According to the characterization by Alamdari et al. [1], some binary trees have no self-approaching drawings in $\mathbb{R}^2$. We show that this is no longer the case in $\mathbb{H}^2$.

Theorem 4. *Let $T = (V, E)$ be a tree, such that each node of T has degree either 1 or 3. Then, T has a self-approaching drawing in $\mathbb{H}^2$, in which every arc has the same hyperbolic length and every pair of incident arcs forms an angle of* 120°.

Proof. For convenience, we subdivide each edge of T once. We shall show that both pieces are collinear in the resulting drawing Γ and have the same hyperbolic length.

First, consider a regular hexagon $\hexagon = p_0p_1p_2p_3p_4p_5$ centered at the origin o of D; see Fig. 6a. In $\mathbb{H}^2$, it can have angles smaller than 120°. We choose them to be 90° (any angle between 0° and 90° would work). Next, we draw a $K_{1,3}$ with center v_0 in o and the leaves v_1, v_2, v_3 in the middle of the arcs p_0p_1, p_2p_3, p_4p_5 respectively.

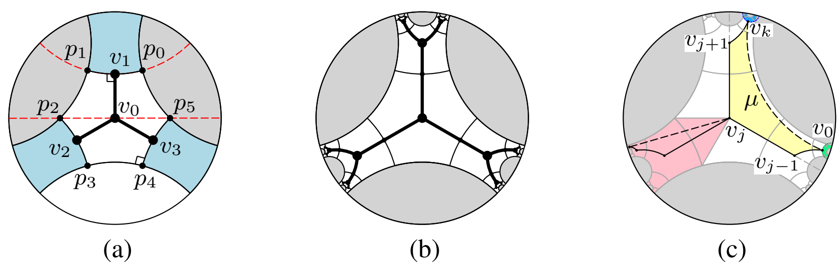

Fig. 6: Constructing increasing-chord drawings of binary trees and cactuses in $\mathbb{H}^2$.

For each such building block of the drawing consisting of a $K_{1,3}$ inside a regular hexagon with $90°$ angles, we add its copy mirrored at an arc of the hexagon containing a leaf node of the tree constructed so far. For example, in the first iteration, we add three copies of $\hexagon$ mirrored at p_0p_1, p_2p_3 and p_4p_5, respectively, and the corresponding inscribed $K_{1,3}$ subtrees. The construction after two iterations is shown in Fig. 6b. This process can be continued infinitely to construct a drawing Γ_∞ of the infinite binary tree. However, we stop after we have completed Γ for the tree T.

We now show that Γ_∞ (and thus also Γ) has the desired properties. Due to isometries and the aforementioned sufficient condition, it suffices to consider edge $e = v_0v_1$ and show that a normal on e does not cross Γ_∞ in another point. To see this, consider Fig. 6a. Due to the choice of the angles of $\hexagon$, all the other hexagonal tiles of Γ_∞ are contained in one of the three blue quadrangular regions $\square_i := l^+_{v_0v_i} \setminus (l^+_{v_ip_{2i-1}} \cup l^+_{v_ip_{2i-2}})$, $i = 1, 2, 3$. Thus, the regions $l^+_{v_1p_1}$ and $l^+_{v_1p_0}$ (gray) contain no point of Γ_∞. Therefore, since each normal on v_0v_1 is contained in the "slab" $D \setminus (l^+_{v_0v_1} \cup l^+_{v_1v_0})$ bounded by the diameter through p_2, p_5 and the line through p_0, p_1 (dashed) and is parallel to both of these lines, it contains no other point of Γ_∞. □

We note that our proof is similar in spirit to the one by Kleinberg [12], who also used tilings of $\mathbb{H}^2$ to prove that any tree has a greedy drawing in $\mathbb{H}^2$.

As in the Euclidean case, it can be easily shown that if a tree T contains a node v of degree 4, it has a self-approaching drawing in $\mathbb{H}^2$ if and only if T is a subdivision of $K_{1,4}$ (apply an isometry, such that v is in the origin of D). This completely characterizes the trees admitting a self-approaching drawing in $\mathbb{H}^2$. Further, it is known that every binary cactus and, therefore, every 3-connected planar graph has a binary spanning tree [5, 13].

Corollary 2. (i) *A tree T has an increasing-chord drawing in $\mathbb{H}^2$ if and only if T either has maximum degree 3 or is a subdivision of $K_{1,4}$.* (ii) *Every binary cactus and, therefore, every 3-connected planar graph has an increasing-chord drawing in $\mathbb{H}^2$.*

Again, note that this is not the case for binary cactuses in $\mathbb{R}^2$; see the example in Theorem 2. We use the above construction to produce *planar* self-approaching drawings of binary cactuses in $\mathbb{H}^2$. We show how to choose a spanning tree and angles at vertices of degree 2, such that non-tree edges can be added without introducing crossings; see Fig. 6c for a sketch and the full version [15] for the proof.

Corollary 3. *Every binary cactus has a planar increasing-chord drawing in* $\mathbb{H}^2$.

References

1. S. Alamdari, T. M. Chan, E. Grant, A. Lubiw, and V. Pathak. Self-approaching graphs. In W. Didimo and M. Patrignani, editors, *Graph Drawing (GD'12)*, vol. 7704 of *LNCS*, pages 260–271. Springer, 2013.
2. P. Angelini, E. Colasante, G. Di Battista, F. Frati, and M. Patrignani. Monotone drawings of graphs. *J. Graph Algorithms Appl.*, 16(1):5–35, 2012.
3. P. Angelini, G. Di Battista, and F. Frati. Succinct greedy drawings do not always exist. *Networks*, 59(3):267–274, 2012.
4. P. Angelini, W. Didimo, S. Kobourov, T. Mchedlidze, V. Roselli, A. Symvonis, and S. Wismath. Monotone drawings of graphs with fixed embedding. In M. Kreveld and B. Speckmann, editors, *Graph Drawing (GD'11)*, vol. 7034 of *LNCS*, pages 379–390. Springer, 2012.
5. P. Angelini, F. Frati, and L. Grilli. An algorithm to construct greedy drawings of triangulations. *J. Graph Algorithms Appl.*, 14(1):19–51, 2010.
6. R. Dhandapani. Greedy drawings of triangulations. *Discrete Comput. Geom.*, 43:375–392, 2010.
7. D. Eppstein and M. T. Goodrich. Succinct greedy geometric routing using hyperbolic geometry. *IEEE Trans. Computers*, 60(11):1571–1580, 2011.
8. S. Felsner. Geometric Graphs and Arrangements. Vieweg+Teubner Verlag, 2004.
9. M. T. Goodrich and D. Strash. Succinct greedy geometric routing in the Euclidean plane. In Y. Dong, D.-Z. Du, and O. Ibarra, editors, *Algorithms and Computation (ISAAC'09)*, vol. 5878 of *LNCS*, pages 781–791. Springer, 2009.
10. W. Huang, P. Eades, and S.-H. Hong. A graph reading behavior: Geodesic-path tendency. In *IEEE Pacific Visualization Symposium (PacificVis'09)*, pages 137–144, 2009.
11. C. Icking, R. Klein, and E. Langetepe. Self-approaching curves. *Math. Proc. Camb. Phil. Soc*, 125:2001, 1995.
12. R. Kleinberg. Geographic routing using hyperbolic space. In *Computer Communications (INFOCOM'07)* , pages 1902–1909, 2007. IEEE.
13. A. Moitra and T. Leighton. Some Results on Greedy Embeddings in Metric Spaces. *Discrete Comput. Geom.*, 44:686–705, 2010.
14. M. Nöllenburg and R. Prutkin. Euclidean greedy drawings of trees. In H. Bodlaender and G. Italiano, editors, *Algorithms (ESA'13)*, vol. 8125 of *LNCS*, pages 767–778. Springer, 2013.
15. M. Nöllenburg, R. Prutkin, and I. Rutter. On Self-Approaching and Increasing-Chord Drawings of 3-Connected Planar Graphs. CoRR arXiv:1409.0315 (2014)
16. C. H. Papadimitriou and D. Ratajczak. On a conjecture related to geometric routing. *Theor. Comput. Sci.*, 344(1):3–14, 2005.
17. H. C. Purchase, J. Hamer, M. Nöllenburg, and S. G. Kobourov. On the usability of Lombardi graph drawings. In W. Didimo and M. Patrignani, editors, *Graph Drawing (GD'12)*, vol. 7704 of *LNCS*, pages 451–462. Springer, 2013.
18. A. Rao, S. Ratnasamy, C. Papadimitriou, S. Shenker, and I. Stoica. Geographic routing without location information. In *Mobile Computing and Networking (MobiCom '03)*, pages 96–108, 2003. ACM.
19. G. Rote. Curves with increasing chords. *Math. Proc. Camb. Phil. Soc*, 115:1–12, 1 1994.
20. W. Schnyder. Embedding planar graphs on the grid. In *Discrete Algorithms (SODA '90)*, pages 138–148, 1990. SIAM.
21. J.-J. Wang and X. He. Succinct strictly convex greedy drawing of 3-connected plane graphs. *Theor. Comput. Sci.*, 532(0):80 – 90, 2014.